

---

# Statistical Measures For Defining Curriculum Scoring Function

---

Vinu Sankar Sadasivan<sup>1</sup> Anirban Dasgupta<sup>1</sup>

## Abstract

Curriculum learning is a training strategy that sorts the training examples by some measure of their difficulty and gradually exposes them to the learner to improve the network performance. Motivated by our insights from implicit curriculum ordering, we first introduce a simple curriculum learning strategy that uses statistical measures such as standard deviation and entropy values to score the difficulty of data points for real image classification tasks. We empirically show its improvements in performance with convolutional and fully-connected neural networks on multiple real image datasets. We also propose and study the performance of a dynamic curriculum learning algorithm. Our dynamic curriculum algorithm tries to reduce the distance between the network weight and an optimal weight at any training step by greedily sampling examples with gradients that are directed towards the optimal weight. Further, we use our algorithms to discuss why curriculum learning is helpful.

of the ability to generalize (Shirish Keskar & Socher, 2017). Hence, SGD still remains one of the main workhorses of the machine learning optimization toolkit.

SGD proceeds by stochastically making unbiased estimates of the gradient on the full data (Zhao & Zhang, 2015). However, this approach does not match the way humans typically learn various tasks. We learn a concept faster if we are presented easy examples first and then gradually exposed to examples with more complexity, based on a curriculum. An orthogonal extension to SGD (Weinshall et al., 2018), that has some promise in improving its performance is to choose examples according to a specific strategy, driven by cognitive science – this is curriculum learning (CL) (Bengio et al., 2009), wherein the examples are shown to the learner based on a curriculum.

In this work, we propose two novel approaches for CL – a practical algorithm that uses statistical measures for scoring examples and setting up curricula for image datasets, and a toy dynamic curriculum learning (DCL) framework. We do a thorough empirical study of our practical algorithm and provide some more insights into why CL works. Our contributions are as follows:

## 1. Introduction

Stochastic Gradient Descent (SGD) (Robbins & Monro, 1951) is a simple yet widely used algorithm for machine learning optimization. There have been many efforts to improve its performance. A number of such directions, such as AdaGrad (Duchi et al., 2011), RMSProp (Tieleman & Hinton, 2012), and Adam (Kingma & Ba, 2015), improve upon SGD by fine-tuning its learning rate, often adaptively. However, Wilson et al. (2017) has shown that the solutions found by adaptive methods generalize worse even for simple overparameterized problems. Reddi et al. (2018) introduced AMSGrad hoping to solve this issue. Yet there is performance gap between AMSGrad and SGD in terms

- We introduce a **simple, novel, and practical CL approach for image classification tasks that does the ordering of examples in an unsupervised manner using statistical measures**. Our insight is that statistical measures could have an association with implicit curricula ordering. We empirically analyze our argument of using statistical scoring measures (especially standard deviation) over combinations of multiple datasets and networks.
- We propose a novel dynamic curriculum learning (DCL) algorithm to study the behaviour of CL. DCL is not a practical CL algorithm since it requires the knowledge of a reasonable local optima to compute the gradients of the full data after every training epoch. DCL uses the **gradient information to define a curriculum that minimizes the distance between the current weight and a desired local minima after every epoch**. However, this simplicity in the definition of DCL makes it easier to analyze its performance formally.

---

<sup>1</sup>Department of Computer Science & Engineering, Indian Institute of Technology Gandhinagar, Gujarat, India. Correspondence to: Vinu Sankar Sadasivan <vinu.sankar@alumni.iitgn.ac.in>.



Figure 1. Implicit curricula: Top and bottom rows contain images that are learned at the beginning and end of the training, respectively. Top rows: CIFAR-100, bottom rows: MNIST.

- Our DCL algorithm generates a natural ordering for training the examples. Previous CL works have demonstrated that exposing a part of the data initially and then gradually exposing the rest is a standard way to setup a curriculum. We use two variants of our DCL framework to show that **it is not just the subset of data which is exposed to the model that matters, but also the ordering within the data partition that is exposed.**
- We analyze how **DCL is able to serve as a regularizer and improve the generalization of networks.** Additionally, we study why CL based on standard deviation scoring works using our DCL framework.

### 1.1. Related Works

Bengio et al. (2009) formalizes the idea of CL in machine learning framework where the examples are fed to the learner in an order based on its *difficulty*. The notation of difficulty scoring of examples has not really been formalized and various heuristics have been tried out: Bengio et al. (2009) uses manually crafted scores, self-paced learning (SPL) (Kumar et al., 2010) uses the loss values with respect to the learner’s current parameters, and CL by transfer learning (Hacohen & Weinshall, 2019) uses the loss values with respect to a pre-trained model to rate the difficulty of examples in a dataset. Among these works, what makes SPL particular is that they use a dynamic CL strategy, i.e., the preferred ordering is determined dynamically over the course of the optimization. However, SPL does not really improve the performance of deep learning models, as noted in (Fan et al., 2018). Similarly, Loshchilov & Hutter (2015) uses a function of rank based on latest loss values for online batch selection for faster training of neural networks. Katharopoulos & Fleuret (2018) and Chang et al. (2017) perform importance sampling to reduce the variance of stochastic gradients during training. Graves et al. (2017) and Matiisen et al. (2019) propose teacher-guided

automatic CL algorithms that employ various supervised measures to define dynamic curricula. The most recent works in CL show its advantages in reinforcement learning (Portelas et al., 2020; Zhang et al., 2020).

The recent work by Weinshall et al. (2018) introduces the notion of *ideal difficulty score* to rate the difficulty of examples based on their loss values with respect to a set of optimal hypotheses. They theoretically show that for linear regression, the expected rate of convergence at a training step for an example monotonically decreases with its ideal difficulty score. This is practically validated by Hacohen & Weinshall (2019) by sorting the training examples based on the performance of a network trained through transfer learning. They also show that anti-curriculum learning, exposing the most difficult examples first, leads to a degrade in the network performance. However, there is a lack of theory to show that CL improves the performance of a completely trained network. Thus, while CL indicates that it is possible to improve the performance of SGD by a judicious ordering, both theoretical insights as well as concrete empirical guidelines to create this ordering remain unclear. In contrast to CL (Hacohen & Weinshall, 2019), anti-curriculum learning (Kocmi & Bojar, 2017; Zhang et al., 2018; Zhang et al., 2019) can be better than CL in certain settings.

Hacohen et al. (2020) and Wu et al. (2021) investigate *implicit curricula* and observe that networks learn examples in a dataset in a highly consistent order. Figure 1 shows the implicit order in which a convolutional neural network (CNN) learns data points from MNIST and CIFAR-100 datasets. Wu et al. (2021) also shows that CL (*explicit curriculum*) can be useful in scenarios with limited training budget or noisy data. Mirzasoileiman et al. (2020) uses a coreset construction method to dynamically expose a subset of the dataset to robustly train neural networks against noisy labels.

While the previous CL works employ tedious methods to score the difficulty level of the examples, Hu et al. (2020) uses the number of audio sources to determine the difficulty for audiovisual learning. Liu et al. (2020) uses the norm of word embeddings as a difficulty measure for CL for neural machine translation. In light of these recent works, we discuss the idea of using statistical measures to score examples making it easy to perform CL on real image datasets without the aid of any pre-trained network.

## 2. Preliminaries

At any training step  $t$ , SGD updates the current weight  $w_t$  using  $\nabla f_i(w_t)$  which is the gradient of loss of example  $x_i$  with respect to the current weight. The learning rate and the data are denoted by  $\eta$  and  $\mathcal{X} = \{(x_i, y_i)\}_{i=0}^{N-1}$ , respectively, where  $x_i \in [-1, 1]^d$  denotes an example and

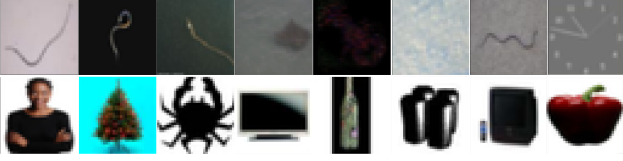


Figure 2. Top 8 images with the lowest standard deviation values (top row) and top 8 images with the highest standard deviation values (bottom row) in CIFAR-100 dataset.

---

**Algorithm 1** Curriculum learning method.
 

---

**Input:** Data  $\mathcal{X}$ , batch size  $b$ , number of mini-batches  $T$ , scoring function  $score$ , and pacing function  $pace$ .

**Output:** Sequence of mini-batches  $[B_0, B_1, \dots, B_{T-1}]$ . sort  $\mathcal{X}$  according to  $score$ , in ascending order.

$B \leftarrow []$

**for**  $i = 0$  to  $T - 1$  **do**

$size \leftarrow pace(i)$

$\tilde{\mathcal{X}}_i \leftarrow \mathcal{X}[0, 1, \dots, size - 1]$

    uniformly sample  $B_i$  of size  $b$  from  $\tilde{\mathcal{X}}_i$

**end for**

**return**  $B$

---

$y_i \in [K]$  its corresponding label for a dataset with  $K$  classes. Without loss of generality, we assume that the dataset is normalized such that  $\sum_{i=0}^{N-1} \mathbf{x}_i = \mathbf{0}$ . We denote the learner as  $h_\vartheta : [-1, 1]^d \rightarrow [K]$ . Generally, SGD is used to train  $h_\vartheta$  by giving the model a sequence of mini-batches  $\{B_0, B_1, \dots, B_{T-1}\}$ , where  $B_i \subseteq \mathcal{X} \forall i \in [T]$ . Traditionally, each  $B_i$  is generated by uniformly sampling examples from the data. We denote this approach as *vanilla*.

In CL, the curriculum is defined by two functions, namely the scoring function and the pacing function. The scoring function,  $score_\vartheta(\mathbf{x}_i, y_i) : [-1, 1]^d \times [K] \rightarrow \mathbb{R}$ , scores each example in the dataset. Scoring function is used to sort  $\mathcal{X}$  in an ascending order of difficulty. A data point  $(\mathbf{x}_i, y_i)$  is said to be easier than  $(\mathbf{x}_j, y_j)$  if  $score_\vartheta(\mathbf{x}_i, y_i) < score_\vartheta(\mathbf{x}_j, y_j)$ , where both the examples belong to  $\mathcal{X}$ . Unsupervised scoring measures do not use the data labels to determine the difficulty of data points. The pacing function,  $pace_\vartheta(t) : [T] \rightarrow [N]$ , determines how much of the data is to be exposed at a training step  $t \in [T]$ .

### 3. Statistical measures for defining curricula

In this section, we discuss our simple approach of using statistical measures to define curricula for real image classification tasks. Hacoheh et al. (2020) shows that the orders in which a dataset is learned by various network architectures are highly correlated. While training a stronger learner, it first learns the examples learned by a weaker learner, and then continues to learn new examples. Can we design an

explicit curriculum that sorts the examples according to the implicit order in which they are learned by a network? From Figure 1 it is clear that the CIFAR-100 images learned at the beginning of training have bright backgrounds or rich color shades, while the images learned at the end of training have monotonous colors. We observe that the CIFAR-100 images learned at the beginning of training have a higher mean standard deviation ( $= 0.25$ ) than those learned at the end of training ( $= 0.19$ ). For MNIST, the mean standard deviation of images learned at the beginning of training ( $= 0.23$ ) is lesser than those learned at the end of training ( $= 0.25$ ). Motivated by this observation, we investigate the benefits of using standard deviation for defining curriculum scoring functions in order to improve the generalization of the learner. We perform multiple experiments and validate our proposal over various image classification datasets with different network architectures.

Standard deviation and entropy are informative statistical measures for images and used widely in digital image processing (DIP) tasks (Kumar & Gupta, 2012; Arora, 1981). Mastriani & Giraldez (2016) uses standard deviation filters for effective edge-preserving smoothing of radar images. Natural images might have a higher standard deviation if they have a lot of edges and/or vibrant range of colors. Edges and colours are among the most important features that help in image classification at a higher level. Figure 2 shows 8 images which have the lowest and highest standard deviations in the CIFAR-100 dataset. Entropy gives a measure of image information content and is used for various DIP tasks such as automatic image annotation (Jeon & Manmatha, 2004).

We experiment using the standard deviation measure (*stddev*), the Shannon’s entropy measure (*entropy*) (Shannon, 1951), and different norm measures as scoring functions for CL (see Algorithm 1). The performance improvement with norm measures is not consistent and significant over the experiments we perform (see Suppl. A for details). For a flattened image example represented as  $\mathbf{x}_i = [x_i^{(0)}, x_i^{(1)}, \dots, x_i^{(d-1)}]^T \in [-1, 1]^d$ , we define

$$\mu(\mathbf{x}_i) = \frac{\sum_{j=0}^{d-1} x_i^{(j)}}{d} \quad \text{and} \quad (1)$$

$$stddev(\mathbf{x}_i) = \sqrt{\frac{\sum_{j=0}^{d-1} (x_i^{(j)} - \mu(\mathbf{x}_i))^2}{d}}.$$

We use a fixed exponential pace function that exponentially increases the amount of data exposed to the network after every fixed *step\_length* number of training steps. For a training step  $i$ , it is formally given as:  $pace(i) = \lfloor \min(1, starting\_fraction \cdot inc^{\lfloor \frac{i}{step\_length} \rfloor}) \cdot N \rfloor$ , where *starting\_fraction* is the fraction of the data that is exposed to the model initially, *inc* is the exponential factor by which the the pace function value increases after a step, and  $N$  is

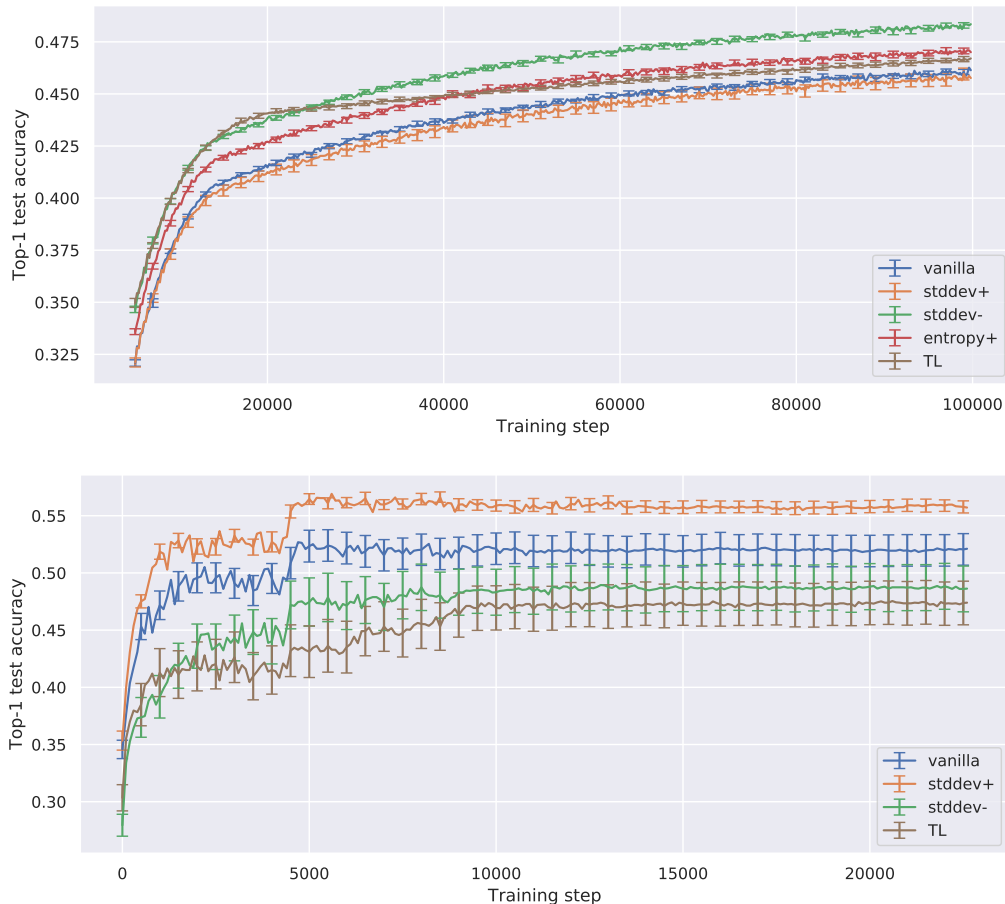


Figure 3. Learning curves for Cases 3 (top row: CNN-8 + CIFAR-100) and 4 (bottom row: CNN-8 + ImageNet Cats). Error bars represent the standard error of the mean (STE) after 25 and 10 independent trials.

the total number of examples in the data.

### 3.1. Baselines

We use *vanilla* and CL by transfer learning (Hacohen & Weinshall, 2019), denoted as *TL*, as our baselines. We use the same hyperparameters and the codes<sup>1</sup> published by the authors for running *TL* experiments. *TL* works with the aid of an Inception network (Szegedy et al., 2016a) pre-trained on the ImageNet dataset (Deng et al., 2009). The activation levels of the penultimate layer of this Inception network is used as a feature vector for each of the images in the training data. These features are used to train a classifier (e.g, support vector machine) and its confidence scores for each of the training images are used as the curriculum scores.

<sup>1</sup>[https://github.com/GuyHacohen/curriculum\\_learning](https://github.com/GuyHacohen/curriculum_learning)

### 3.2. Experiments

We denote CL models with scoring functions *stddev* as *stddev+*,  $-stddev$  as *stddev-*, *entropy* as *entropy+*, and  $-entropy$  as *entropy-*. Our codes are published on GitHub<sup>2</sup>. We employ three network architectures for our experiments: a) FCN-512 – A 2-layer fully-connected network (FCN- $m$ ) with  $m = 512$  hidden neurons with Exponential Linear Unit (ELU) nonlinearities, b) CNN-8 (Hacohen & Weinshall, 2019) – A moderately deep CNN with 8 convolution layers and 2 fully-connected layers, and c) ResNet-20 (He et al., 2016) – A deep CNN.

We use the following datasets for our experiments: a) MNIST, b) Fashion-MNIST, c) CIFAR-10, d) CIFAR-100, e) Small Mammals (a super-class of CIFAR-100, (Krizhevsky et al., 2009)), and f) ImageNet Cats (a subset of 7 classes of cats in ImageNet, see Suppl. B.3). For our experiments, we use the same setup as used in Hacohen & Weinshall (2019). We use learning rates with an

<sup>2</sup>[https://github.com/vinusankars/curriculum\\_learning](https://github.com/vinusankars/curriculum_learning)



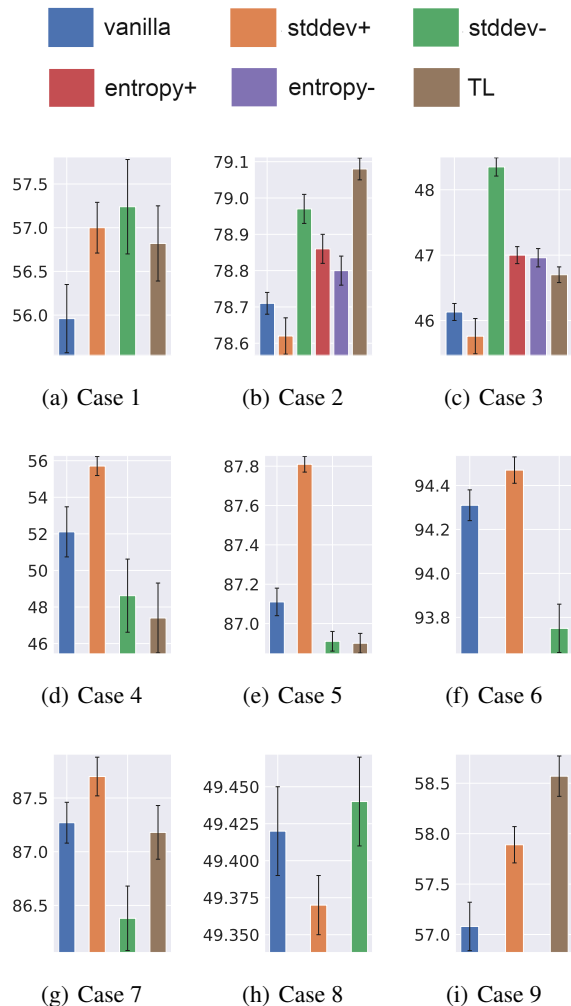


Figure 4. Bars represent the final mean top-1 test accuracy (in %) achieved by models in Cases 1–9. Error bars represent the STE after 25 independent trials for Cases 2, 3, 5 – 8, and 10 independent trials for Cases 1, 4, 9.

exponential step-decay rate for the optimizers in all our experiments as traditionally done (Simonyan & Zisserman, 2015; Szegedy et al., 2016b). In all our experiments, the models use fine-tuned hyperparameters for the purpose of an unbiased comparison of model generalization over the test set. More experimental details are deferred to Suppl. B. While practically performing model training, we prioritize class balance. Although we do not follow the exact ordering provided by the curriculum scoring function, the ordering within a class is preserved.

We define 9 test cases. Cases 1–5 use CNN-8 to classify Small Mammals, CIFAR-10, CIFAR-100, ImageNet Cats, and Fashion-MNIST datasets, respectively. Cases 6–8 use FCN-512 to classify MNIST, Fashion-MNIST, and CIFAR-10 datasets, respectively. Case 9 uses ResNet-20 to classify the ImageNet Cats dataset.

Table 1. *stddev* curriculum selection using median pixel distance values. Bolded value corresponds to the curriculum variant that works the best for a dataset.

DATASET	$M_+$	$M_-$
MNIST	<b>0.01</b>	0.00
FASHION-MNIST	<b>0.06</b>	0.01
SMALL MAMMALS	0.03	<b>0.08</b>
CIFAR-10	0.02	<b>0.06</b>
CIFAR-100	0.06	<b>0.09</b>
IMAGENET CATS	<b>0.07</b>	0.02

Figure 3 shows the improvement in network generalization of CNN-8 on CIFAR-100 and ImageNet Cats datasets using *stddev* CL algorithms. Figure 4 shows the results of all the test cases that we perform. From Figures 4(b) and 4(c) it is clear that *stddev* serves as a better scoring function than *entropy*. Further, we observe that the datasets MNIST, Fashion-MNIST, and ImageNet Cats best follow the curriculum variant *stddev+*. CIFAR-100, CIFAR-10, and Small Mammals follow the curriculum defined by *stddev-*. As discussed earlier in this section, this trend is consistent with the *stddev* order in which the dataset images are implicitly learned by the network. In all the test cases, *stddev* CL algorithm consistently performs better than *vanilla* with a mean improvement of  $\sim 1.05\%$  top-1 test accuracy.

Let  $med(\mathbf{x})^3$  denote the median value of all the pixels in image(s)  $\mathbf{x}$  and  $M = med([\mathbf{x}_i]_{i=0}^{N-1})$  denote the median pixel value of the full training images, where the examples are ordered according to *stddev+*. We denote  $M_+ = |M - med([\mathbf{x}_i]_{i=0}^{b-1})|$  and  $M_- = |M - med([\mathbf{x}_i]_{i=N-1-b}^{N-1})|$  as the median pixel distances of the first batches of examples sampled according to *stddev+* and *stddev-*, respectively, where  $b$  is the batch size. Interestingly, we notice that the *stddev* curriculum variant that best works for a dataset has a higher median pixel distance as shown in Table 1.

<sup>3</sup>Similar to NumPy median function.

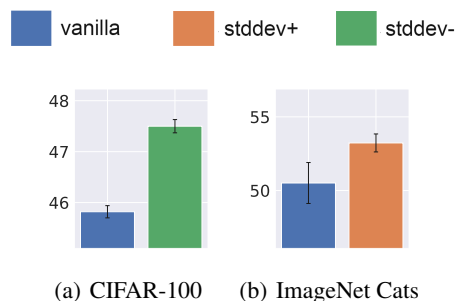


Figure 5. Bars represent the final mean top-1 test accuracy (in %) achieved by CNN-8. Error bars represent the STE after 25 and 10 independent trials, respectively.

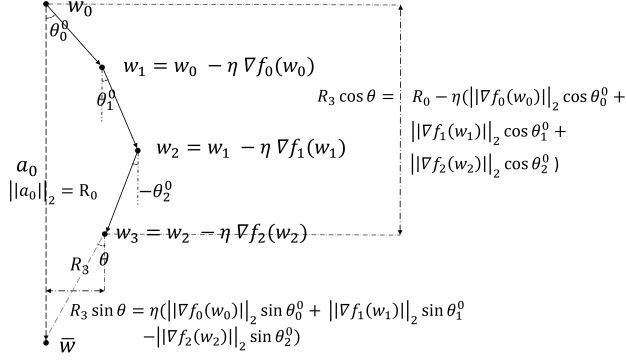


Figure 6. A geometrical interpretation of gradient steps for the understanding of equation 2.

---

**Algorithm 2** Dynamic curriculum learning (*DCL+*).

**Input:** Data  $\mathcal{X}$ , local minima  $\bar{w}$ , weight  $w_t$ , batch size  $b$ , and pacing function *pace*.

**Output:** Sequence of mini-batches  $B_t$  for the next training epoch.

$\mathbf{a}_t \leftarrow \bar{w} - w_t$

$\rho_t \leftarrow []$

$B_t \leftarrow []$

**for**  $i = 0$  **to**  $N - 1$  **do**

$$\rho_{t,i} \leftarrow -\frac{\mathbf{a}_t^\top \cdot \nabla f_i(w_t)}{\|\mathbf{a}_t\|_2}.$$

**end for**

$\mathcal{X}_t \leftarrow \mathcal{X}$  sorted according to  $\rho_{t,i}$ , in ascending order

$size \leftarrow pace(t)$

**for** ( $i = 0$ ;  $size$ ;  $b$ ) **do**

append  $\mathcal{X}_t[i, \dots, i + b - 1]$  to  $B_t$

**end for**

**return**  $B_t$

---

We also test the robustness of our *stddev* algorithms to noisy labels. For this purpose, we design two test cases: CNN-8 to classify CIFAR-100 and ImageNet Cats datasets with 20% label noise. We add label noise by uniformly sampling 20% of the data points and randomly changing their labels. Figure 5 shows that our CL algorithms work well in training settings with label noise, even with only coarse fine-tuning of curriculum hyperparameters.

## 4. Dynamic Curriculum Learning

For DCL algorithms (Kumar et al., 2010), examples are either scored and sorted or automatically selected (Graves et al., 2017; Matiisen et al., 2019) after every few training steps since the scoring function changes dynamically with the learner as training proceeds. Hacothen & Weinshall (2019) and Bengio et al. (2009) use a fixed scoring function and pace function for the entire training process. They empirically show that a curriculum helps to learn fast in

the initial phase of the training process. In this section, we propose our novel DCL algorithm for studying the behaviour of CL. Our DCL algorithm updates the difficulty scores of all the examples in the training data at every epoch using their gradient information.

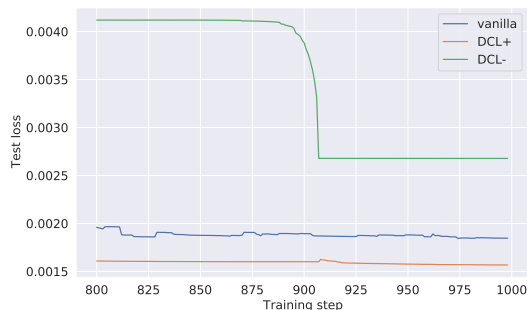
We hypothesize the following: Given a weight initialization  $w_0$  and a local minima  $\bar{w}$  obtained by full training of *vanilla* SGD, the curriculum ordering determined by our DCL variant leads to convergence in fewer number of training steps than *vanilla*. We first describe the algorithm, then the underlying intuition, and finally validate the hypothesis using experiments.

Our DCL algorithm iteratively works on reducing the L2 distance,  $R_t$ , between the weight parameters  $w_t$  and  $\bar{w}$  at any training step  $t$ . Suppose,  $S_t$  is the index of the example sampled at training step  $t$ , and for any  $\tilde{t} < t$ ,  $S_{\tilde{t},t}$  is the ordered set containing the  $(t - \tilde{t} + 1)$  indices of training examples that are to be shown to the learner from the training steps  $\tilde{t}$  through  $t$ . Let us define  $\mathbf{a}_t = (\bar{w} - w_t)$ ,  $R_t = \|\mathbf{a}_t\|_2$ , and  $\theta_t^i$  as the angle between  $\nabla f_{S_t}(w_t)$  and  $\mathbf{a}_t$ . Then, using a geometrical argument, (see Figure 6),

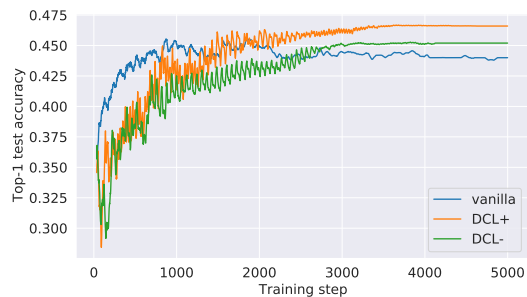
$$\begin{aligned} R_t^2 &= \left( R_{\tilde{t}} - \eta \sum_{j=\tilde{t}}^{j=t-1} \left( \|\nabla f_{S_j}(w_j)\|_2 \cos \theta_j^{\tilde{t}} \right) \right)^2 \\ &\quad + \eta^2 \left( \sum_{j=\tilde{t}}^{j=t-1} \left( \|\nabla f_{S_j}(w_j)\|_2 \sin \theta_j^{\tilde{t}} \right) \right)^2 \\ &= R_{\tilde{t}}^2 - 2\eta R_{\tilde{t}} \sum_{j=\tilde{t}}^{j=t-1} \left( \|\nabla f_{S_j}(w_j)\|_2 \cos \theta_j^{\tilde{t}} \right) \\ &\quad + \eta^2 \left( \sum_{j=\tilde{t}}^{j=t-1} \left( \|\nabla f_{S_j}(w_j)\|_2 \cos \theta_j^{\tilde{t}} \right) \right)^2 \\ &\quad + \eta^2 \left( \sum_{j=\tilde{t}}^{j=t-1} \left( \|\nabla f_{S_j}(w_j)\|_2 \sin \theta_j^{\tilde{t}} \right) \right)^2 \end{aligned} \quad (2)$$

For a *vanilla* model,  $S_{0,T}$  is generated by uniformly sampling indices from  $[N]$  with replacement. Since, finding an ordered set  $S_{0,T}$  to minimize  $R_T^2$  is computationally expensive, we approximate the DCL algorithm (*DCL+*, see Algorithm 2) by neglecting the terms with coefficient  $\eta^2$  in equation 2. Algorithm 2 uses a greedy approach to approximately minimize  $R_t^2$  by sampling examples at every epoch using the scoring function

$$\begin{aligned} score_{\tilde{t}}(\mathbf{x}_{S_t}) &= -\|\nabla f_{S_t}(w_t)\|_2 \cos \theta_t^{\tilde{t}} \\ &= -\frac{\mathbf{a}_t^\top \cdot \nabla f_{S_t}(w_t)}{\|\mathbf{a}_t\|_2} = \rho_{\tilde{t},S_t}. \end{aligned} \quad (3)$$



(a) Experiment 1



(b) Experiment 2

Figure 7. Learning curves of experiments comparing *DCL+*, *DCL-*, and *vanilla* SGDs.

Let us denote the models that use the natural ordering of mini-batches greedily generated by Algorithm 2 as *DCL+*. *DCL-* uses the same sequence of mini-batches that *DCL+* exposes to the network at any given epoch, but the order is reversed. We empirically show that *DCL+* achieves a faster and better convergence with various initializations of  $w_0$ .

#### 4.1. Experiments

In our experiments, we set  $pace(t) = \lfloor kN \rfloor \forall t$ , where  $k \in [b/N, 1]$  is a tunable hyperparameter. We use FCN-10 architecture to empirically validate our algorithms ( $k = 0.9$ ) on a subset of the MNIST dataset with class labels 0 and 1 (Experiment 1). Since, this is a very easy task (as the *vanilla* model training accuracy is as high as  $\sim 99.9\%$ ), we compare the test loss values across training steps in Figure 7(a) to see the behaviour of DCL on an easy task. *DCL+* shows the fastest convergence, although all the networks achieve the same test accuracy. *DCL+* achieves *vanilla*'s final (at training step 1000) test loss score at training step 682.

In Experiment 2, we use FCN-128 to evaluate our DCL algorithms ( $k = 0.6$ ) on a relatively difficult Small Mammals dataset. Figure 7(b) shows that *DCL+* achieves a faster and better convergence than *vanilla* in Experiment 2. *DCL+*

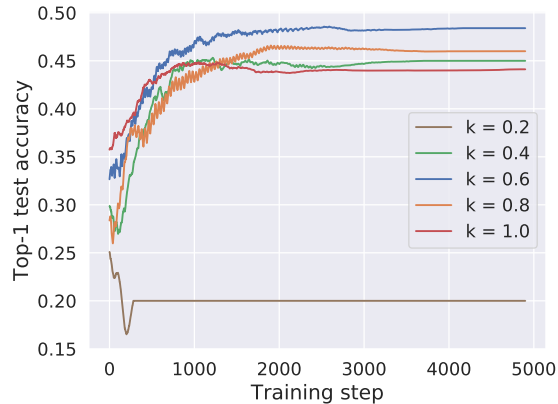


Figure 8. Learning curves for Experiment 2 with varying  $pace(t) = \lfloor kN \rfloor$  for *DCL+*. The parameter  $k$  needs to be finely tuned for improving the generalization of the network. A low  $k$  value exposes only examples with less/no gradient noise to the network at every epoch whereas a high  $k$  value exposes most of the dataset including examples with high gradient noise to the network. A moderate  $k$  value shows examples with low/moderate gradient noise. Here, a moderate  $k = 0.6$  generalizes the best.

achieves *vanilla*'s convergence (at training step 4900) test accuracy score at training step 1896. Further experimental details are deferred to Suppl. B.1.

Since, DCL is computationally expensive, we perform DCL experiments only on small datasets. Fine-tuning of  $k$  is crucial for improving the generalization of *DCL+* on the test set (see Figure 8). We fine-tune  $k$  by trial-and-error over the training accuracy score.

### 5. Why is a curriculum useful?

At an intuitive level, we can say that *DCL+* converges faster than the *vanilla* SGD as we greedily sample those examples whose gradient steps are the most aligned towards an approximate optimal weight vector. In previous CL works, mini-batches are generated by uniformly sampling examples from a partition of the dataset which is made by putting a threshold on the difficulty scores of the examples. Notice that our DCL algorithms generate mini-batches with a natural ordering at every epoch. We design *DCL+* and *DCL-* to investigate an important question: can CL benefit from having a set of mini-batches with a specific order or is it just the subset of data that is exposed to the learner that matters? Figure 7 shows that the ordering of mini-batches matters while comparing *DCL+* and *DCL-*, which expose the same set of examples to the learner in any training epoch. Once the mini-batch sequence for an epoch is computed, *DCL-* provides mini-batches to the learner in the decreasing order of gradient noise. This is the reason for *DCL-* to have high discontinuities in the test loss curve after every epoch in Figure 7(a). With our empirical results, we argue that the



Figure 9. Relation of  $\rho$  and  $stddev$  values of examples over training epochs 1 (left), 5 (middle), and 100 (right) for Experiments 1 (top row) and 2 (bottom row), respectively. Dotted red lines fit the scattered points.

### ordering of mini-batches within an epoch does matter.

Bengio et al. (2009) illustrates that removing examples that are misclassified by a Bayes classifier (*noisy* examples) provides a good curriculum for training networks. SPL tries to remove examples that might be misclassified during a training step by avoiding examples with high loss. *TL* avoids examples that are noisy to an approximate optimal hypotheses in the initial phases of training. *DCL+* and *DCL-* try to avoid examples with *noisy gradients* that might slow down the convergence towards the desired optimal minima. Guo et al. (2018) empirically shows that avoiding examples with label noise improves the initial learning of CNNs. According to their work, adding examples with label noise to later phases of training serves as a regularizer and improves the generalization capability of CNNs. *DCL+* uses its pace function to avoid highly noisy examples (in terms of gradients). In our DCL experiments, the parameter  $k$  is chosen such that few moderately noisy examples (examples present in the last few mini-batches within an epoch) are included in training along with lesser noisy examples to improve the network’s generalization. We also show the importance of tuning CL hyperparameters for achieving a better network generalization (see Figure 8). Hence, the parameter  $k$  in *DCL+* serves as a regularizer and helps in improving the generalization of networks.

#### 5.1. Analyzing $stddev$ with our DCL framework

We use our DCL framework to understand why  $stddev$  works as a scoring function. We try to analyze the relation between the standard deviation and  $\rho_{t,i}$  values of examples over training epochs. Figure 9 shows the plots of  $stddev$  on the Y-axis against examples ranked based on their  $\rho_{t,i}$  values (in as-

cending order) plotted on the X-axis at various stages of training. It shows the dynamics of  $\rho_{t,i}$  over initial, intermediate, and final stages of training. Correlation between  $\rho_{t,i}$  and  $stddev$  after the first epoch for Experiments 1 and 2 are 0.74 and 0.36, respectively. The corresponding p-values for testing non-correlation are 0 and  $3 \times 10^{-79}$ , respectively. In the initial stage of training, examples with high  $stddev$  tend to have high  $\rho$  values. In the final stage of training, this trend changes to the exact opposite. This shows that  $stddev$  can be useful in removing noisy gradients from the initial phases of training and hence help in defining a simple, good curriculum.

## 6. Conclusion

In this paper, we propose two novel CL algorithms that show improvements in network generalization over multiple image classification tasks with CNNs and FCNs. A fresh approach to define curricula for image classification tasks based on statistical measures is introduced, based on our observations from implicit curricula ordering. This technique makes it easy to score examples in an unsupervised manner without the aid of any teacher network. We thoroughly evaluate our CL algorithms and find it beneficial in noisy settings and improving network accuracy. We also propose a novel DCL algorithm for analyzing CL. We show that the ordering of mini-batches within training epochs and fine-tuning of CL hyperparameters are important to achieve good results with CL. Further, we also use our DCL framework to support our CL algorithm that uses  $stddev$  for scoring examples.



## References

- Arora, P. On the shannon measure of entropy. *Information Sciences*, 23(1):1–9, 1981.
- Bengio, Y., Louradour, J., Collobert, R., and Weston, J. Curriculum learning. In *Proceedings of the 26th annual international conference on machine learning*, pp. 41–48, 2009.
- Chang, H.-S., Learned-Miller, E., and McCallum, A. Active bias: Training more accurate neural networks by emphasizing high variance samples. In Guyon, I., Luxburg, U. V., Bengio, S., Wallach, H., Fergus, R., Vishwanathan, S., and Garnett, R. (eds.), *Advances in Neural Information Processing Systems*, volume 30, pp. 1002–1012. Curran Associates, Inc., 2017.
- Deng, J., Dong, W., Socher, R., Li, L., Kai Li, and Li Fei-Fei. Imagenet: A large-scale hierarchical image database. In *2009 IEEE Conference on Computer Vision and Pattern Recognition*, pp. 248–255, 2009.
- Duchi, J., Hazan, E., and Singer, Y. Adaptive subgradient methods for online learning and stochastic optimization. *Journal of machine learning research*, 12(7), 2011.
- Fan, Y., Tian, F., Qin, T., Li, X.-Y., and Liu, T.-Y. Learning to teach. In *International Conference on Learning Representations*, 2018.
- Graves, A., Bellemare, M. G., Menick, J., Munos, R., and Kavukcuoglu, K. Automated curriculum learning for neural networks. In *International Conference on Machine Learning*, pp. 1311–1320. PMLR, 2017.
- Guo, S., Huang, W., Zhang, H., Zhuang, C., Dong, D., Scott, M. R., and Huang, D. Curriculumnet: Weakly supervised learning from large-scale web images. In *Proceedings of the European Conference on Computer Vision (ECCV)*, pp. 135–150, 2018.
- Hacohen, G. and Weinshall, D. On the power of curriculum learning in training deep networks. In *International Conference on Machine Learning*, pp. 2535–2544. PMLR, 2019.
- Hacohen, G., Choshen, L., and Weinshall, D. Let’s agree to agree: Neural networks share classification order on real datasets. In *International Conference on Machine Learning*, pp. 3950–3960. PMLR, 2020.
- He, K., Zhang, X., Ren, S., and Sun, J. Deep residual learning for image recognition. In *2016 IEEE Conference on Computer Vision and Pattern Recognition (CVPR)*, pp. 770–778, 2016.
- Hu, D., Wang, Z., Xiong, H., Wang, D., Nie, F., and Dou, D. Curriculum audiovisual learning. *arXiv preprint arXiv:2001.09414*, 2020.
- Jeon, J. and Manmatha, R. Using maximum entropy for automatic image annotation. In *International Conference on Image and Video Retrieval*, pp. 24–32. Springer, 2004.
- Katharopoulos, A. and Fleuret, F. Not all samples are created equal: Deep learning with importance sampling. In *International conference on machine learning*, pp. 2525–2534. PMLR, 2018.
- Kingma, D. P. and Ba, J. Adam: A method for stochastic optimization. In Bengio, Y. and LeCun, Y. (eds.), *3rd International Conference on Learning Representations, ICLR 2015, San Diego, CA, USA, May 7-9, 2015, Conference Track Proceedings*, 2015.
- Kocmi, T. and Bojar, O. Curriculum learning and minibatch bucketing in neural machine translation. In *Proceedings of the International Conference Recent Advances in Natural Language Processing, RANLP 2017*, pp. 379–386, Varna, Bulgaria, September 2017. INCOMA Ltd.
- Krizhevsky, A., Hinton, G., et al. Learning multiple layers of features from tiny images. 2009.
- Kumar, M. P., Packer, B., and Koller, D. Self-paced learning for latent variable models. In *NIPS*, volume 1, pp. 2, 2010.
- Kumar, V. and Gupta, P. Importance of statistical measures in digital image processing. *International Journal of Emerging Technology and Advanced Engineering*, 2(8): 56–62, 2012.
- Liu, X., Lai, H., Wong, D. F., and Chao, L. S. Norm-based curriculum learning for neural machine translation. In *Proceedings of the 58th Annual Meeting of the Association for Computational Linguistics*, pp. 427–436, 2020.
- Loshchilov, I. and Hutter, F. Online batch selection for faster training of neural networks. *ArXiv*, abs/1511.06343, 2015.
- Mastriani, M. and Giraldez, A. E. Enhanced directional smoothing algorithm for edge-preserving smoothing of synthetic-aperture radar images. *arXiv preprint arXiv:1608.01993*, 2016.
- Matiisen, T., Oliver, A., Cohen, T., and Schulman, J. Teacher–student curriculum learning. *IEEE Transactions on Neural Networks and Learning Systems*, 31(9):3732–3740, 2019.
- Mirzasoleiman, B., Cao, K., and Leskovec, J. Coresets for robust training of deep neural networks against noisy

- labels. In *Advances in Neural Information Processing Systems*, 2020.
- Portelas, R., Colas, C., Hofmann, K., and Oudeyer, P.-Y. Teacher algorithms for curriculum learning of deep rl in continuously parameterized environments. In *Conference on Robot Learning*, pp. 835–853. PMLR, 2020.
- Reddi, S. J., Kale, S., and Kumar, S. On the convergence of adam and beyond. In *International Conference on Learning Representations*, 2018.
- Robbins, H. and Monro, S. A stochastic approximation method. *The annals of mathematical statistics*, pp. 400–407, 1951.
- Shannon, C. E. Prediction and entropy of printed english. *Bell system technical journal*, 30(1):50–64, 1951.
- Shirish Keskar, N. and Socher, R. Improving generalization performance by switching from adam to sgd. *arXiv e-prints*, pp. arXiv–1712, 2017.
- Simonyan, K. and Zisserman, A. Very deep convolutional networks for large-scale image recognition. In Bengio, Y. and LeCun, Y. (eds.), *3rd International Conference on Learning Representations, ICLR 2015, San Diego, CA, USA, May 7-9, 2015, Conference Track Proceedings*, 2015.
- Szegedy, C., Vanhoucke, V., Ioffe, S., Shlens, J., and Wojna, Z. Rethinking the inception architecture for computer vision. In *Proceedings of the IEEE conference on computer vision and pattern recognition*, pp. 2818–2826, 2016a.
- Szegedy, C., Vanhoucke, V., Ioffe, S., Shlens, J., and Wojna, Z. Rethinking the inception architecture for computer vision. In *Proceedings of the IEEE conference on computer vision and pattern recognition*, pp. 2818–2826, 2016b.
- Tieleman, T. and Hinton, G. Lecture 6.5-rmsprop: Divide the gradient by a running average of its recent magnitude. *COURSERA: Neural networks for machine learning*, 4 (2):26–31, 2012.
- Weinshall, D., Cohen, G., and Amir, D. Curriculum learning by transfer learning: Theory and experiments with deep networks. In *International Conference on Machine Learning*, pp. 5238–5246. PMLR, 2018.
- Wilson, A. C., Roelofs, R., Stern, M., Srebro, N., and Recht, B. The marginal value of adaptive gradient methods in machine learning. In *Proceedings of the 31st International Conference on Neural Information Processing Systems*, pp. 4151–4161, 2017.
- Wu, X., Dyer, E., and Neyshabur, B. When do curricula work? In *International Conference on Learning Representations*, 2021.
- Zhang, X., Kumar, G., Khayrallah, H., Murray, K., Gwinup, J., Martindale, M. J., McNamee, P., Duh, K., and Carpuat, M. An Empirical Exploration of Curriculum Learning for Neural Machine Translation. *arXiv e-prints*, art. arXiv:1811.00739, November 2018.
- Zhang, X., Shapiro, P., Kumar, G., McNamee, P., Carpuat, M., and Duh, K. Curriculum learning for domain adaptation in neural machine translation. In *Proceedings of the 2019 Conference of the North American Chapter of the Association for Computational Linguistics: Human Language Technologies, Volume 1 (Long and Short Papers)*, pp. 1903–1915. ACL, June 2019.
- Zhang, Y., Abbeel, P., and Pinto, L. Automatic curriculum learning through value disagreement. *Advances in Neural Information Processing Systems*, 33, 2020.
- Zhao, P. and Zhang, T. Stochastic optimization with importance sampling for regularized loss minimization. In *International Conference on Machine Learning*, pp. 1–9. PMLR, 2015.

## Supplementary Material

### A. Additional empirical results

In Section 3, we study the performance of CL using *stddev* and *entropy* as scoring measures. Other important statistical measures are mode, median, and norm (Kumar & Gupta, 2012). A high *stddev* for a real image could mean that the image is having a lot of edges and a wide range of colors. A low entropy could mean that an image is less noisy. Norm of an image could give information about its brightness. Intuitively, norm is not a good measure for scoring images as low norm valued images are really dark and high norm valued images are really bright. We experiment with different norm measures and find that they do not serve as a good CL scoring measure since they have lesser improvement with high variance over multiple trials when compared to *stddev* on the CIFAR datasets. We use two norm measures:

$$\begin{aligned} \text{norm}(\mathbf{x}) &= \|\mathbf{x}\|_2 & \text{and} \\ \text{class\_norm}(\mathbf{x}) &= \|\mathbf{x} - \mu_{\mathbf{x}}\|_2, \end{aligned} \quad (4)$$

where  $\mathbf{x}$  is an image in the dataset represented as a vector, and  $\mu_{\mathbf{x}}$  is the mean pixel value of all the images belonging to the class of  $\mathbf{x}$ . In our experiments, all the orderings are performed based on the scoring function and the examples are then arranged to avoid class imbalance within a mini-batch. Let us denote the models that use the scoring functions *norm* as *norm+*,  $-norm$  as *norm-*, *class\_norm* as *class\_norm+*, and  $-class\_norm$  as *class\_norm-*.

Figure 10 shows the results of our experiments on CIFAR-100 and CIFAR-10 datasets with CNN-8 using *norm* and *class\_norm* scoring functions. We find that

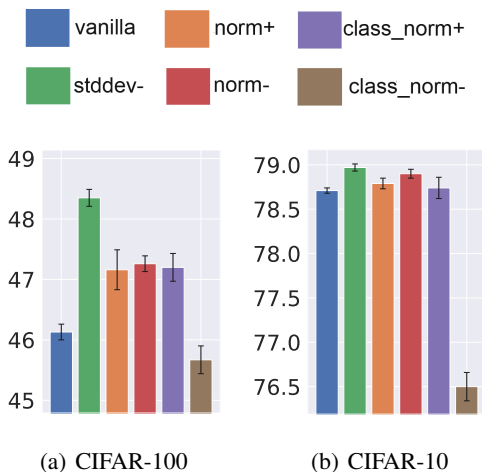


Figure 10. Bars represent the final mean top-1 test accuracy (in %) achieved by CNN-8. Error bars represent the STE after 25 independent trials.

the improvements reported for *norm-*, the best model among the models that use norm measures, have a lower improvement than *stddev-*. Also, *norm-* has a higher STE when compared to both *vanilla* and *stddev-*. Hence, based on our results, we suggest that *stddev* is a more useful statistical measure than norm measures for defining curricula for image classification tasks.

### B. Experimental Details

#### B.1. Network architectures

All FCNs (denoted as FCN- $m$ ) we use are 2-layered with a hidden layer consisting of  $m$  neurons with ELU nonlinearities. Experiment 1 employs FCN-10 while Experiment 2 employs FCN-128 with no bias parameters. The outputs from the last layer is fed into a softmax layer. Cases 6–8 employ FCN-512 with bias parameters. The batch-size for Experiments 1–2 and Cases 1–9 are 50 and 100, respectively. We use one NVIDIA Quadro RTX 5000 GPU for our experiments. Average runtimes of our experiments vary from 1 hour to 3 days.

For Cases 1–5 and 9, we use the CNN-8 architecture that is used in Hacoheh & Weinshall (2019). The codes are available in their GitHub repository. CNN-8 contains 8 convolution layers with 32, 32, 64, 64, 128, 128, 256, and 256 filters, respectively, and ELU nonlinearities. Except for the last two convolution layers with filter size  $2 \times 2$ , all other layers have a filter size of  $3 \times 3$ . Batch normalization is performed after every convolution layer.  $2 \times 2$  max-pooling and 0.25 dropout layers are present after every two convolution layers. The output from the CNN is flattened and fed into a fully-connected layer with 512 neurons followed by a 0.5 dropout layer. A softmax layer follows the fully-connected output layer that has a number of neurons same as the number of classes in the dataset. The batch-size is 100. All the CNNs and FCNs are trained using SGD with cross-entropy loss. SGD uses an exponential step-decay learning rate scheduler. Our codes will be published on acceptance.

#### B.2. Hyperparameter tuning

For fair comparison of network generalization, the hyperparameters should be finely tuned as mentioned in Hacoheh & Weinshall (2019). We exploit hyperparameter grid-search to tune the hyperparameters of the models in our experiments. For *vanilla* models, grid-search is easier since they do not have a pace function. For CL models, we follow a coarse two-step tuning process as they have a lot of hyperparameters. First we tune the optimizer hyperparameters fixing other CL hyperparameters. Then we fix the obtained optimizer parameters and tune the CL hyperparameters.

The grid-search parameter ranges are as follows. Case 1: a)

initial learning rate 0.01 – 0.1 b) learning rate exponential decay factor 1.1 – 2 c) learning rate decay step 200 – 800 d) *step\_length* 20 – 400 e) *inc* 1.1 – 3 f) *starting\_fraction* 0.04 – 0.15. Cases 2–3, 9: a) initial learning rate 0.05 – 0.2 b) learning rate exponential decay factor 1.1 – 2 c) learning rate decay step 200 – 800 d) *step\_length* 100 – 2000 e) *inc* 1.1 – 3 f) *starting\_fraction* 0.04 – 0.15. Case 4–5, 9: a) initial learning rate 0.005 – 0.5 b) learning rate exponential decay factor 2 – 10 c) learning rate decay step 100 – 12000 d) *step\_length* 10 – 100 e) *inc* 1.1 – 2 f) *starting\_fraction* 0.04 – 0.15. Cases 6–8: a) initial learning rate 0.001 – 0.01 b) learning rate exponential decay factor 1.1 – 2 c) learning rate decay step 200 – 800 d) *step\_length* 20 – 100 e) *inc* 1.1 – 2 f) *starting\_fraction* 0.04 – 0.15. The experiments are tuned to perform better on the training data.

### B.3. Dataset details

We use CIFAR-100, CIFAR-10, ImageNet Cats, Small Mammals, MNIST, and Fashion-MNIST datasets. CIFAR-100 and CIFAR-10 contain 50,000 training and 10,000 test images of shape  $32 \times 32 \times 3$  belonging to 100 and 10 classes, respectively. Small Mammals is a super-class of CIFAR-100 containing 5 classes – “Hamster”, “Mouse”, “Rabbit”, “Shrew”, and “Squirrel”. It has 500 training images per class and 100 test images per class. MNIST and Fashion-MNIST contain 60,000 training and 10,000 test gray-scale images of shape  $28 \times 28$  belonging to 10 different classes. ImageNet Cats is a subset of the ImageNet dataset ILSVRC 2012. It has 7 classes with each class containing 1300 training images and 50 test images. The labels in the subset are “Tiger cat”, “Lesser panda, Red panda, Panda, Bear cat, Cat bear, Ailurus fulgens”, “Egyptian cat”, “Persian cat”, “Tabby, Tabby cat”, “Siamese cat, Siamese”, “Madagascar cat”, and “Ring-tailed lemur, Lemur catta”. The images in the dataset are reshaped to  $56 \times 56 \times 3$ . All the datasets are preprocessed before training to have a zero mean and unit standard deviation.